Tunable Diode Laser and Difference Frequency Generation Absorption Spectrometers for Highly Sensitive Airborne Measurements of Trace Atmospheric Constituents

Alan Fried[*a], Petter Weibring[a], Dirk Richter[a], James Walega[a], Chad Roller[b], and Frank Tittel[c]
[a]The National Center for Atmospheric Research, Boulder, Colorado, 80301
[b]Ekips Technologies, Norman, Oklahoma, 73069
[c]Rice University Quantum Institute, Houston, Texas, 77005-1892

ABSTRACT

Enhancing our understanding of atmospheric processes and transformations require a suite of ever more sensitive, selective, versatile, and fast instruments that can measure trace atmospheric constituents at and below mixing ratios of 100-parts-per-trillion on airborne platforms. Instruments that can carry out such measurements are very challenging, as airborne platforms vibrate, experience accelerations, and undergo large swings in cabin temperatures and pressures. These challenges notwithstanding, scientists and engineers at the National Center for Atmospheric Research (NCAR) in collaboration with Rice University have long been employing mid-infrared absorption spectroscopy to acquire atmospheric measurements of important trace gases like formaldehyde on a variety of airborne platforms. The present paper will discuss two very recent airborne formaldehyde instruments employing tunable diode laser and difference frequency generation mid-IR laser sources. Both instruments employ second-harmonic absorption spectroscopy utilizing astigmatic multipass Herriott cells. This paper will discuss the performance of both instruments during recent airborne campaigns, focusing on the many steps necessary for minimizing the various aircraft perturbations. Prospects for the detection of other trace gases will also be presented.

Keywords: formaldehyde, atmospheric trace gas detection, airborne measurements, tunable diode laser measurements, difference frequency generation

1. INTRODUCTION

The technique of tunable diode laser absorption spectroscopy has been widely employed in the laboratory and on ground-based, airborne, and balloon-borne, platforms to study atmospheric processes and transformations. The fundamentals of this technique as well as the numerous trace gases studied are presented in a recent review book chapter by Fried and Richter [1]. This book chapter also discusses a relatively new variant of this technique employing difference frequency generation (DFG) laser sources in place of the more traditional liquid-nitrogen cooled lead-salt diode laser. The National Center for Atmospheric Research (NCAR) and Rice University have established a close collaboration to further pursue and develop this exciting new technology for mid-infrared absorption spectrometers. This paper will present a brief overview of both approaches, with specific emphasis on airborne platforms. Although this discussion focuses on airborne measurements of formaldehyde, an important trace gas of interest to our collective laboratories over the past decade [2-8], the conclusions are widely applicable to many other trace gases.

Formaldehyde (CH_2O) is a ubiquitous component of both the remote atmosphere as well as the polluted urban atmosphere. This important gas-phase intermediate is a primary emission product from hydrocarbon combustion sources as well as from oxidation of natural hydrocarbons emitted by plants and trees. Through its subsequent decomposition by photolysis and reaction with the hydroxyl (OH) radical, CH_2O serves as a source of the hydroperoxy radical (HO_2) and carbon monoxide (CO). In producing HO_2, CH_2O affects the partitioning among odd hydrogen radicals (HO_x = [H] + [OH] + [HO_2]), which through their rapid reactions with hydrocarbons control the oxidation capacity of the atmosphere. Radical production from CH_2O becomes particularly relevant at high solar zenith angles and in the mid to upper troposphere, where other sources of odd hydrogen radicals become less important. Finally, as many hydrocarbon oxidation reactions proceed through CH_2O as an intermediate, CH_2O becomes important in further testing our understanding of hydrocarbon reaction mechanisms. Highly accurate measurements of CH_2O throughout the mid to upper troposphere are thus important for improving our understanding of tropospheric photochemistry.

Chemical and Biological Sensors for Industrial and Environmental Monitoring II
edited by Steven D. Christesen, Arthur J. Sedlacek III, James B. Gillespie, Kenneth J. Ewing
Proc. of SPIE Vol. 6378, 63780F, (2006) · 1605-7422/06/$15 · doi: 10.1117/12.691318

Because of its broad range of sources, ambient CH_2O mixing ratios attain levels as high as several tens of parts-per-billion (ppbv, where 1 ppbv is 1 part in 10^9) in urban areas to levels as low as tens of parts-per-trillion (pptv, where 1 pptv is 1 part in 10^{12}) in the remote background atmosphere. In the latter case, ambient measurements become quite challenging, particularly on airborne platforms where fast measurements (seconds to minutes) are required and severe vibrations and variable sampling conditions of temperature, pressure, and relative humidity are encountered. The present paper will present a comparison of two mid-infrared absorption spectrometers employing: 1) a more traditional liquid-nitrogen cooled tunable lead salt diode laser; and 2) a relatively new difference frequency generation (DFG) laser source. For facility of discussion, the former spectrometer will hereafter be referred to as a tunable diode laser absorption spectrometer (TDLAS) and the latter as a difference frequency generation absorption spectrometer (DFGAS). Both spectrometers employ the same data acquisition/processing approaches with major exception, and this will be discussed in the DFGAS section.

1.1 Airborne Tunable Diode Laser Absorption Spectrometer

The airborne TDLAS has undergone numerous upgrades and improvements over the years and the latest version is described in detail in references [6, 8] and schematically depicted in Figure 1. Only a brief overview of the technical details will be discussed here.

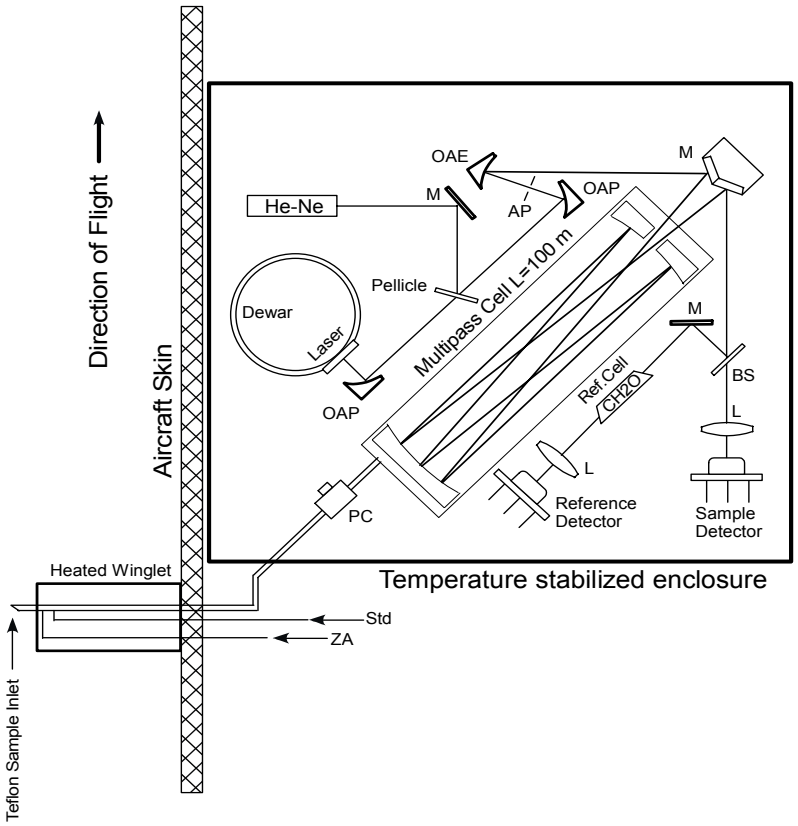

Figure 1: Schematic of airborne tunable diode laser system for measurements of CH_2O. The components are as follows: PC (pressure controller); OAP (off axis parabolic mirror); OAE (off axis ellipsoidal mirror); M (flat mirror); AP (aperture); L (lens); BS (beam splitter); Std (CH_2O gas-phase calibration standard injection line); and ZA (zero air addition line). Cell flow is maintained using a vacuum pump (not shown) attached to the cell outlet port located beneath the input/output beam on the right-hand side of the figure.

The infrared radiation (3.5-μm) from the liquid-nitrogen cooled lead salt diode laser is directed through a multi-pass astigmatic Herriott absorption cell (Aerodyne Incorporated, 100-meter optical pathlength and 3-liter volume) using a series of off-axis and flat mirrors. The cell output beam is imaged onto cryogenically cooled InSb sample and reference detectors. The reference detector arm contains a reference cell with pure CH_2O at 10-Torr, which is used for wavelength locking (to be discussed). The entire optical system, including the optical bench, is mounted inside a temperature stabilized optical enclosure, achieved by circulating air through fin-type heaters mounted in the lid. The enclosure material was a commercial product (Gilfab) constructed by sandwiching an insulating balsa wood core between two thin sheets of aluminum. Temperature control becomes extremely important when operating on an aircraft where cabin temperatures can dramatically change by as much as 15 °C over the duration of an 8 – 10 hour flight, depending upon location on the aircraft and the particular aircraft. Such large changes cause dramatic changes in optical alignment, which in turn lead to optical noise (to be discussed). At the center of our thermally stabilized enclosure the air temperature is typically stable to within ± 0.2 °C (maximum deviation of 0.7 °C) over the course of a 10-hour flight.

1.2 Data Acquisition

The laser is repetitively tuned across a CH_2O absorption feature at 2831.6417 cm^{-1} by sweeping the injection current using a function generator card and a triangle waveform at 25 Hz, which produces 2 scans (up and down) of the laser for each triangle waveform. An additional triangle waveform rapidly modulates the laser at 50 kHz. The detector signals are directed into lock-in amplifiers where the 2*f* (100 kHz) demodulated signals from both channels are determined. The output of the lock-in amplifiers is further co-averaged employing a 16-bit analog-to-digital converter data acquisition card and a computer. The data acquisition card samples at a frequency of 10 kHz (400 points per period of the sweep waveform 200 points per scan) and is triggered with a TTL signal from the function generator card at the beginning of each sweep waveform. Roller et al. [8] discuss the merits of using a triangle sweep ramp over a sawtooth waveform. However, employing a triangle sweep ramp adds some complexity to the data processing; a hysteresis in the laser tuning between the 'up' and 'down' ramps requires data from each ramp to be treated as independent samples using their own respective calibration and background spectra (to be discussed) in the data fitting. In this process a mixing ratio is determined for the 'up' and 'down' ramps and the results are then combined to produce one averaged concentration every second.

The reference arm of the optical train, comprised of the reference cell and detector shown in Fig. 1, provides strong unambiguous high signal-to-noise 2*f* CH_2O absorption spectra that can be used in real time to correct for laser wavelength drifts between scans before co-averaging. Various research groups have successfully employed a number of strategies for this purpose involving either the application of a feedback signal to the laser temperature or current controllers or the shifting of acquired spectra in memory before co-averaging. Our airborne system incorporates a combination of both strategies: we utilize fast shifting in memory employing the absorption line center to co-align each scan before co-averaging and the application of feedback current to the laser controller at the end of each background-ambient-background acquisition sequence (to be discussed) to keep the absorption feature centered in the scan window. As discussed by Roller et al. [8] an autocorrelation routine is used in the case of the former.

Ambient air is continuously drawn through the Herriott cell at flow rates of 8 – 10 standard liters per minute (slm, where standard conditions are defined as T = 273.15 K and P = 760 Torr) employing a 1.3-cm OD PFA Teflon line mounted in the heated winglet structure shown. The winglet protrudes outside the aircraft boundary layer and faces perpendicular to the aircraft flow. The winglet structure allows us to heat the inlet line to 35 °C to within a cm of the inlet entrance as well as add zero air to nearly the entire inlet. An oil free scroll pump is used to generate the flow through the gas cell and inlet. An inlet pressure controller, which employs a standard capacitance manometer pressure transducer mounted on the cell, is used to control the cell pressure at around 50 Torr. Zero air (ambient air with CH_2O scrubbed out) generated with a commercial scrubber (manufacture: Advanced Analytical Device Company) and calibration standards are directed into the inlet near the tip using separate addition ports. For zeroing, the scrubbed airflow is switched into the inlet at a flow rate a few slm higher than the cell flow. During calibration, CH_2O standards from permeation devices are introduced into the inlet downstream of the zero air flow using a separate calibration addition port. Calibration spectra are typically collected at CH_2O concentrations of ~ 13 to 14 ppbv, which produces 2*f* absorption signals with high signal-to-noise ratios. Calibration spectra are stored digitally in computer memory for regression fitting for the determination of sample gas mixing ratios.

1.3 Background Subtraction and Optical Noise Reduction

The term "optical noise", as used here, refers collectively to all changes in background structure, and this includes unwanted periodic etalon fringes and less well-defined background structural changes due to small changes in beam alignment, both internal and external to the multipass sampling cell. At the very least, such subtle alignment changes can dramatically affect retrieved concentrations whenever the time evolution of the true background structure does not match the captured background structure acquired during zero air addition (to be discussed). Such alignment changes can also introduce more insidious effects from scattering, which can result in multiple beams impinging upon the sample detector. The result is an undulating background structure comprised of many frequencies, amplitudes, and time constants from multiple scattering sources. To address this, all our airborne measurements employ the technique of rapid background subtraction, which if carried out correctly, significantly reduces the effects of such optical noise structure [see for example ref. 6 and 8]. In this approach spectral background structure is captured by rapidly measuring zero air just prior to and immediately after acquiring ambient sample spectra. Over the years we have employed slightly different variations in the acquisition of background and calibration/ambient spectra. Measurements carried out onboard the NASA DC-8 aircraft during the **In**tercontinental Chemical **T**ransport **Ex**periment- **N**orth **A**merica (INTEX-NA) study in the summer of 2004, background spectra were typically acquired for 15 seconds followed by a 30 second ambient acquisition period or a 30 second calibration acquisition. A second background acquisition period then followed. Between each acquisition switch, the sample cell was flushed with the new sample for ~ 5 seconds before data acquisition was initiated. Each ambient spectral block (flush, pre-background, flush, ambient, flush, post-background) was repeated approximately every 55 to 80 seconds. For facility of discussion, we hereafter refer to each ambient spectral block as a "1-minute average". Subtraction of the pre- and post-backgrounds neighboring the ambient sample spectra are performed using a linear time weighted subtraction (LWS) scheme. The resulting interpolated background spectrum is subtracted point by point over the 200 scan channels from the intervening ambient spectra. The ambient sample spectra in all cases are averaged in 1-second intervals, each average consisting of 25 spectra for both the up and down ramps of the triangle sweep waveform. Obviously 1-second ambient spectra acquired at the start and end of the ambient sequence are most effected by the pre-background and post-backgrounds, respectively.

If the background structure is stable or changes in a smooth linear fashion in time, the background structure is faithfully removed with this LWS procedure. However, in the present airborne system shown in Fig. 1, a number of optical components can cause subtle alignment changes as the cabin pressure is changed and/or the airplane experiences vertical accelerations, with the consequence that the above LWS becomes less valid. Throughout the rest of this paper we refer to such time periods as "Perturbed". The two largest offending components are the Herriott cell and its input window. As discussed by Dyroff et al. [9], dynamic flexure of the Herriott cell end plates and base plate occur as the pressure differential across the cell changes with cabin pressure, and this causes slight misalignment of the cell mirrors. In addition, as the cell window is sealed using a flexible O-ring, the window moves with changing differential pressure. Finally, a number of other components such as the cell input/output flat mirrors and potentially the laser position in the liquid nitrogen dewar can also change due to vertical accelerations. It is important to emphasize that these perturbations are shared by many if not most TDLAS systems, and that the magnitude of such perturbations in the present system is small; during the INTEX-NA study the equivalent line center absorbance magnitude of such perturbations were typically in the 10^{-5} range for 1 second averages. Despite this fact, such optical noise, which may be sufficient for highly polluted conditions (10's of ppbv of CH_2O), is not compatible for measurements of background CH_2O levels in the sub-ppbv range. The latter requires one order of magnitude lower optical noise.

1.4 Data Reduction

CH_2O mixing ratios are determined by fitting the calibration spectrum of known concentration to the sample spectra of unknown concentration using a multiple linear regression approach employing singular value decomposition. The original implementation of this technique in our TDLAS measurements has been described by Sewell et al. [10], and the veracity of the retrieved CH_2O mixing ratios have been repeatedly verified over the years. The linear-least-squares fit is performed on both the 'up' and 'down' scan ramps using a selected fit window to accommodate the absorption feature with sufficient spectral background on both sides for each scan ramp. To accommodate for residual background structure after background subtraction, three background terms (offset, linear and quadratic) are added as basis functions to the regression fit [8,10]. These terms respectively account for a dc offset, a linear slope, and quadratically curved background structure between sample and calibration spectra. During perfect background subtraction these three terms should all be close to zero.

2. AIRBORNE TDLAS SYSTEM PERFORMANCE

2.1 Determination of Limits of Detection During Airborne Operation

Roller et al. [8] and Wert et al. [6] discuss in detail the procedures employed in estimating TDLAS limits of detection (LOD) during airborne operation. Roller et al. [8] found that the best approach was to utilize the replicate precision of the fast measurements (1-second in our case) over many (typically greater than 200) ambient-background acquisition cycles) when the ambient CH_2O mixing ratios were less than 500 pptv. The average 1-second standard deviation so determined over each 1-minute data block was taken as the 1-second LOD (at the 1σ level). The 1-minute LODs were then determined from the 1-second LODs normalized by the square root of 30, the ambient averaging time. This has been verified by select time periods for which replicate 1-minute measurements were indeed low and stable and not affected by instrument perturbations. Allan variance measurements further confirmed the square root of time improvement out to at least 30-seconds. During INTEX-NA this resulted in LOD's of 170 – 290 pptv and 30 – 53 pptv, for the 1-second and 1-minute measurements, respectively.

2.2 TDLAS Optical Perturbations During Airborne Operation

As previously discussed, changes in cabin pressure and vertical accelerations cause a number of optical components to move, resulting in large changes in background structure and degraded performance. Unfortunately, cabin pressure changes are required every time the aircraft undergoes large altitude changes. It is also possible that optical noise generated by scattering outside the absorption cell can change dramatically in structure due to pressure changes in the optical path as illustrated by Fried et al. [11]. Since a typical research flight contains numerous vertical profiles, cabin pressure changes are endemic during airborne operation. In many instances cabin pressure changes and vertical accelerations occur simultaneously as the aircraft altitude is changed. Figure 2 illustrates one example of such perturbations on July 28, 2004.

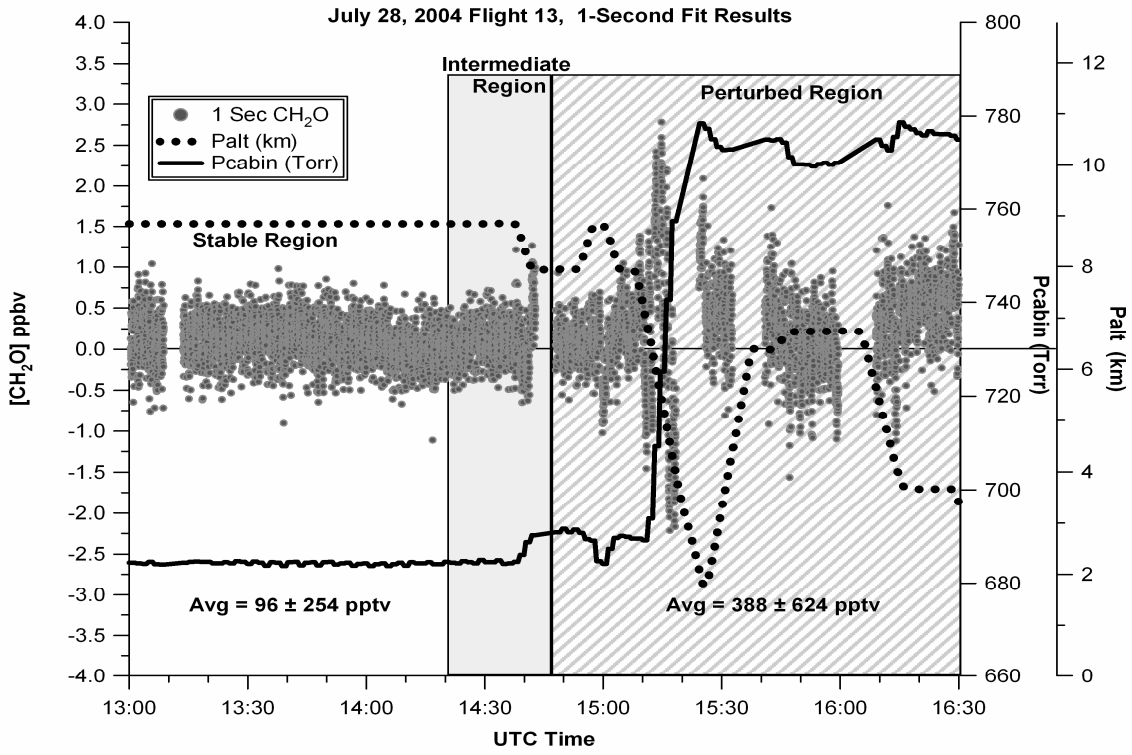

Figure 2: Plot of INTEX-NA 1-second CH_2O measurements on July 28, 2004 showing various stability regions. The average retrieved 1-second CH_2O mixing ratios and the associated standard deviation are given for the Stable and Perturbed regions.

This flight is illustrative of the optical perturbations just discussed; it contains long time periods with vastly different optical behavior. This flight occurred before additional measures were fully implemented to mechanically stabilize the system. Aircraft altitude changes are necessarily accompanied by other aircraft changes; namely, changes in pitch, accelerations, and airspeed. Aircraft cabin pressure was continuously recorded throughout the INTEX-NA mission by a small capacitance monitor mounted on our TDLAS. Here the retrieved fit CH_2O concentrations for combined "up" and "down" ramps for each 1-second measurement are displayed along with the cabin pressure and aircraft altitude (Palt). As is immediately obvious, this figure consists of three stability regions: 1) a "Stable Region" comprised of ~ 1.5 hours of constant altitude flying with constant cabin pressure, constant aircraft speed and constant aircraft pitch; 2) an "Intermediate Region" comprised of ~ 30 minutes of intermediate cabin pressure changes; and 3) a "Perturbed Region" comprised of ~ 2 hours with large perturbations in cabin pressure, and starting at ~ 15:25 and extending through the rest of this period, large continuous changes in both aircraft speed and pitch, necessitated by flying in formation with a much slower aircraft during measurement intercomparisons. It is important to point out that all measurement periods in Fig. 2 were carried over the remote Atlantic Ocean far removed from local pollution sources, as further evidenced by low values for anthropogenic tracers such as carbon monoxide, ethane, and benzene. Hence we can immediately rule out the possibility that the increased measurement scatter in the retrieved CH_2O concentrations during the "Intermediate" and "Perturbed" regions was caused by large ambient variability.

As can be seen, even small cabin pressure changes of ~ 7 Torr in the "Intermediate Region" caused significant optical perturbations and changes in the retrieved 1-second fit concentrations by as much as 1.6 ppbv. During the "Perturbed Region" the cabin pressure changes were much larger, resulting in even larger swings in the retrieved CH_2O concentrations. During these time periods there are frequent breaks in the retrieved data due to the necessity of stopping the acquisition to carry out small alignment changes. Even after these were accomplished, the overall standard deviation for the "Perturbed Region" is still a factor of ~ 3 higher than the "Stable Region". As will be shown, this significantly larger variability signifies a breakdown in the validity of the background LWS and this is further reflected by the fact that acquired backgrounds alternately under-predict and over-predict the true backgrounds underlying each 1-second data point. The Roller et al. study [8] present additional diagnostics highlighting the presence of such perturbations.

The opto-mechanical perturbations just discussed will be present in most airborne TDLAS instruments where multipass absorption cells and other optical windows (detector and dewar windows, for example) exposed to variable differential pressures are employed. Fortunately, we have devised practical solutions to such problems while in the field. First, we addressed the multipass absorption cell. As discussed previously, Dyroff et al. [9] observed dynamic flexure of the Herriott cell end plates and base plate as the pressure differential across the cell changes with cabin pressure, causing slight misalignment of the cell mirrors. In addition, as the cell window is sealed using a flexible O-ring, the window moves with changing differential pressure. Both problems cause large changes in background structure. Dyroff et al. [9] were successful in minimizing the first problem by incorporating four carbon-fiber stabilizing rods on the Herriott cell external structure. Unfortunately, this modification was not possible in the field. A temporary but equally effective solution was implemented in the field by clamping the Herriott cell end plates together with a large commercial pipe clamp. This clamp was positioned and tightened to buck the force exerted by the existing stabilizing rod designed to hold the endplates apart. This effectively reduced changes in the pitch and separation of the cell end plates, and hence cell mirrors, with changing differential pressure. Only slight pressure with the clamp was required to achieve this. Next, we placed an O-ring on the outside of the cell window between the window and the window holder. This O-ring, which was in addition to the sealing O-ring on the cell side of the window, provided enough pressure on the window to minimize window movements with changes in differential pressure across the window. This was accomplished by carefully applying uniform moderate pressure on the window holder after drawing in the window using a vacuum on the cell. The next optical component addressed was the cell input/output mirror mount shown in Fig. 1. Vertical aircraft accelerations produced angular misalignments of the cell input and output beams, which like the other two optical components, resulted in large changes in acquired background spectra. This problem was addressed using a second clamp to compress the spring in the vertical adjustment arm of the mirror mount. The reference arm beam splitter shown in Fig. 1 was also locked in place to avoid small refractive displacements in the sample beam with aircraft accelerations. Finally, the X-Y translator mounts on the first OAP shown in Fig. 1 (the OAP closest to the laser dewar) were locked and the micrometers on both stages were disengaged to avoid coupling in forces to the OAP caused by aircraft accelerations. These improvements in measurement precision are dramatically shown in Figure 3.

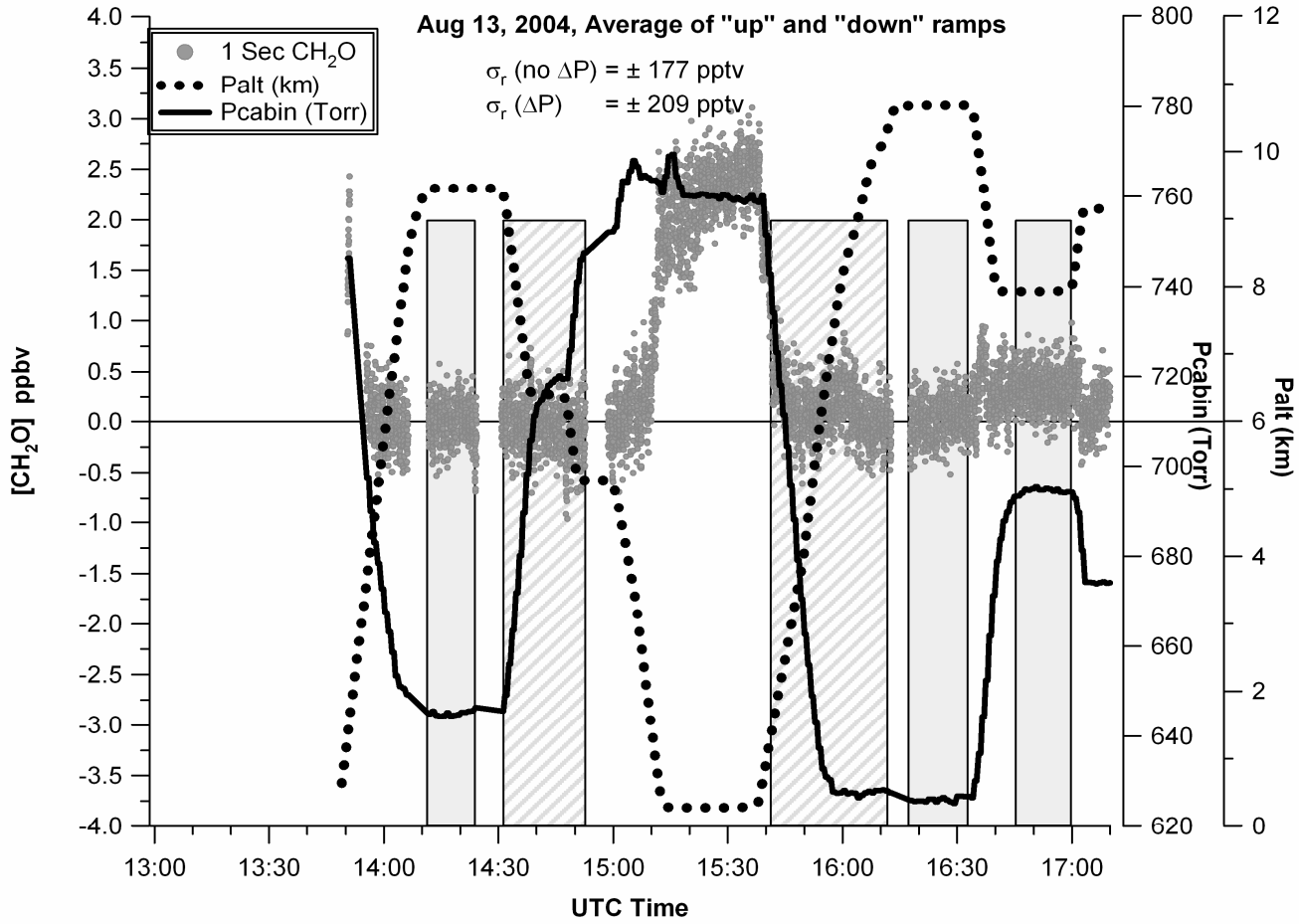

Figure 3: Plot of INTEX-NA 1-second CH_2O measurements on Aug. 13, 2004 after various opto-mechanical issues were addressed.

Figure 3 displays 1-second data for flight 19 acquired on August 13, 2004. Data shown in the crosshatch-shaded blocks were acquired over time periods with cabin pressure changes greater than 100 Torr. In contrast to Fig. 2 where cabin pressure changes of 36 Torr resulted in systematic concentration swings as large as 4.2 ppbv in the retrieved 1-second results, cabin pressure changes greater than 100 Torr in Fig. 3 induced no such systematic swings. The replicate precisions for the data in the two crosshatch shaded blocks (ΔPcabin > 100 Torr) averaged 209 pptv, comparing well with the average value of 177 pptv for the periods shown by the light gray blocks (ΔPcabin < 1.5 Torr). The slight increase of 18% during pressure changes may be associated with real ambient variability. Nevertheless, the behavior shown in Fig. 3 is significantly improved compared to Fig. 2. After these improvements the LODs improved to values around 170 pptv and 30 pptv for the 1-second and 1-minute measurements, respectively. These LOD's were further improved on the subsequent airborne study in 2006. In addition to the measures discussed above, we employed a vertical clamp on the X-Y translator mounts on the first OAP shown in Fig. 1. This further restricted inadvertent movement of the first OAP caused by vertical accelerations. The resulting CH_2O LODs were routine in the range of 120 – 140 pptv and 20 – 30 pptv for the 1-second and 1-minute results, respectively. This corresponds to optical absorbances (base e) of 4×10^{-6} for 1-second measurements, which is equivalent to 4×10^{-10} cm^{-1}.

Although the above performance is quite impressive, considering this was obtained during airborne operation, it is desirable to achieve even lower detection limits by a factor of 3 or more. Unfortunately, it is our belief that TDLAS technology is close to its ultimate performance limit on airborne platforms. The large optical magnification (typically in

the 50 – 100 range) needed in coupling a fast diverging beam into a high f/# Herriott cell places stringent demands on the positional stability of the laser and its relatively massive dewar. Despite the improvements previously discussed, we still observe small but noticeable opto-mechanical perturbations due to aircraft accelerations. These accelerations quite possibly cause the liquid nitrogen cryogen to splash around, affecting the position of the laser mounted in the dewar. For this and the reasons discussed in the next section, we have embarked on the development of a new laser source based upon DFG technology.

3. DFG MEASUREMENTS OF CH_2O

As discussed in our latest DFG study by Weibring et al. [12] and references therein, a fiber pumped DFG source has the potential to significantly improve the performance of airborne CH_2O measurements over TDLAS-based systems. Specific advantages of DFG systems in this regard include: 1) readily available room-temperature single frequency near-infrared pump and signal laser sources; 2) eliminating the need for cryogenic cooling and the associated issues of temperature cycling and concerns about changing laser wavelength and tuning characteristics; 3) eliminating the need of frequent dewar pump-out to reduce the deleterious effects of scattering from condensed dewar contaminants; 4) improved mid-IR laser beam quality, which improves the beam coupling and transmission through the entire optical system, reduces scattering and its associated optical noise, and minimizes the optical alignment effects by cell distortions caused by differential pressure changes across the cell; 5) allows for close coupling of the optical collection element with the PPLN source, which simplifies the transfer optics from the laser source to the multipass absorption cell and reduces required beam magnification, both of which improve the system opto-mechanical stability; 6) eliminating the need for a large and heavy dewar system, which presents challenges in maintaining robust opto-mechanical laser alignment stability, particularly when one experiences cabin pressure changes and/or aircraft accelerations; 7) allows for direct mounting of the DFG stage directly to the absorption cell, which also improves beam pointing stability; 8) allows one to place all the optical components in a small pressure-controlled environment, eliminating beam steering from pressure-induced flexures of the dewar, cell, and detector windows; and 9) allows for a significantly smaller, lighter, more compact, and more versatile multi-species detection system.

Despite these rather significant advantages, the performance of our past CH_2O DFG studies in the laboratory [13, 14] have not been as good as the performance of our airborne TDLAS. In both studies, "fringe-like" optical noise features from the DFG source, which changed over a 1-minute acquisition period, limited the performance. This noise structure in some cases produced an equivalent CH_2O absorbance as large as 1×10^{-3}. Although background subtraction reduced this noise considerably, the results were still less than desired. For example, in the Lancaster et al. study [13], we were only able to achieve 1σ CH_2O detection limits in the 200 – 300 pptv (absorbance sensitivities of $6.7 – 10 \times 10^{-6}$) for 20 – 30 seconds of averaging. The system stability was determined to be only 25 seconds. The Richter et al. [14] study employed a third detector, denoted as the amplitude modulation detector (AMD), to capture the common mode DFG noise structure before the multi-pass cell. Although this improved the resulting performance by a factor of ~ 2, subtle residual differences between the sample and AMD detection chains produced results (1σ 20 second CH_2O detection limits ranging between 86 and 159 pptv) that are still ~ 1 order of magnitude larger than desired. Our latest study by Weibring et al. [12] further investigated the characteristics and temporal response of this large common mode noise feature, and new strategies have been implemented for its effective removal. The ultimate success of these strategies critically depends upon minimizing differential signals between the AMD and cell detector (CD), and this study focuses on the various important factors in this regard. We only present here a brief summary.

The laboratory version of the DFG system is schematically shown in Fig. 4. The laser module is based on two (Signal and Pump) fiber coupled laser sources. A fiber pigtailed DFB diode laser (1562 nm, 70 mW, 360 kHz linewidth) serves as the signal laser, and is controlled by the computer for wavelength scanning, modulation and stabilization. For some experiments, a rare-earth-doped Erbium fiber amplifier was spliced in series with the signal laser to increase the optical input power up to ~ 400 mW. The pump laser source consists of a DFB fiber laser (1083nm, 6mW, 100 kHz linewidth), which is pumped by a Bragg grating stabilized diode laser (974 nm, 130 mW, ~6 GHz linewidth). The output of the fiber laser is spliced to a rare-earth-doped Ytterbium fiber amplifier to increase the power at 1083 nm to 800 mW. The two mixing wavelengths are combined by a low loss wavelength division multiplexer, WDM (loss: 0.05 dB at 1562 nm, 0.13 dB at 1083nm) and spliced to a single mode SMF-28 fiber which connects the pump and signal beams to the DFG stage. The pump and signal beams are launched into the crystal by a two stage lens design, discussed in detail in Richter et al [15]. Briefly, in the first step, a ball lens fused directly to the end of the incoming fiber expands the mode field diameters

of the mixing wavelengths. The focal plane is then re-imaged in a second step by an achromatic lens into the PPLN crystal (l=50mm). This allows for a compact design with improved optical, thermal and mechanical properties. The unconverted signal and pump radiation are removed by a Germanium filter and directed into a beam dump. The passing idler beam is focused by a CaF_2 (f=50 mm) lens and launched into the Herriott cell, yielding a $1/e^2$ focal diameter of ~1.3 mm with a magnification of ~6. The PPLN crystal resides in a Peltier heated copper oven which is temperature stabilized to ~40 ± 0.035 deg °C by a Proportional and Integrating controller (PI). The whole DFG compartment is shielded to avoid scattered light from reaching the detectors. The output beam from the DFG unit is periodically blocked by a shutter to enable detector dark current measurements.

The idler beam, which is scanned across the same isolated and moderately strong CH_2O absorption feature as the TDLAS (2831.6417 cm^{-1}, λ = 3.53 μm), is directed into the multi-pass cell by a gold-coated mirror. As shown in Fig. 4, a tilted and wedged window on the multi-pass cell serves to divert small fractions of the cell input radiation to two different detectors: a detector for wavelength locking (reference detector, RD), and one for removal of optical noise (amplitude modulation detector, AMD). The reflection from the second window surface is routed through a low pressure (10 Torr) cell filled with pure CH_2O and measured by the RD. As in the TDLAS, this RD signal is used for computer controlled wavelength locking. The beam reflected from the first surface of the cell window is focused by an off-axis parabolic mirror onto the AMD, which is used to capture and eliminate common mode optical noise. Two different cell windows were employed. These were made of CaF_2 and Sapphire and yield a reflectivity of ~4% and ~8% respectively. After making 182 passes (~100m) in the cell, the transmitted beam (~ 15 to 18% of the input beam power for the two window materials) emerges from the cell and is collected and imaged by an off-axis parabolic mirror, and focused onto the cell detector (CD). Apertures attached to both focusing optics and detectors minimize the effect of scattered light.

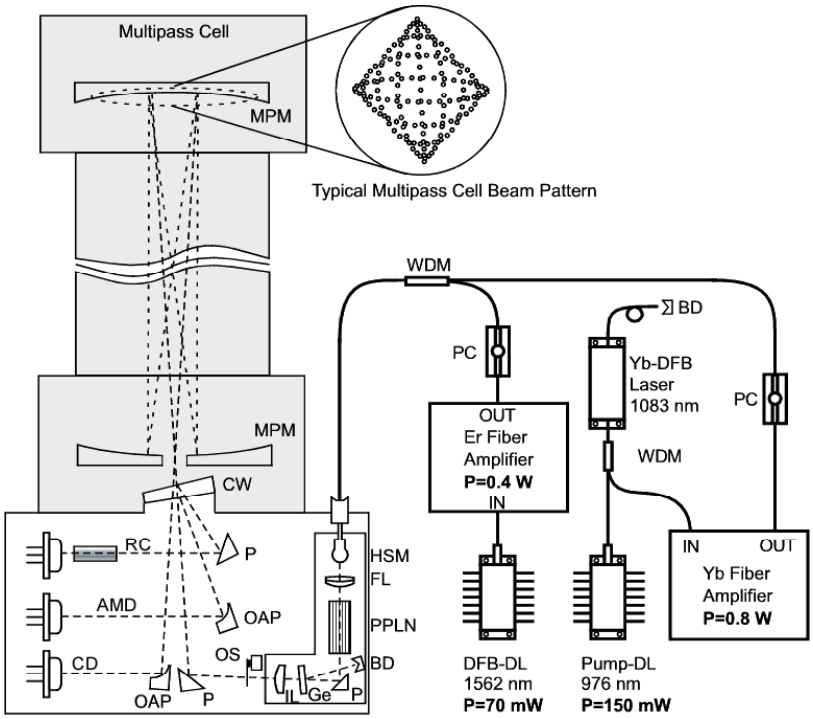

Fig 4. Optical layout of the mid-IR spectrometer. To the right, the laser module consisting of a 976 nm diode laser (Pump-DL), an Ytterbium doped Distributed Feed Back fiber laser (Yb-DFB), an Ytterbium (Yb) fiber amplifier, a 1562 nm (DFB-DL) laser, Polarization controller (PC) and Wavelength division multiplexer (WDM). To the left, the detection module consisting of a Herriott cell and a combined detection unit and difference frequency generation stage. Hybrid Single Mode Fiber (HSM), Focusing Lens (FL) (IL), Beam Dump (BD), Periodically Poled Lithium Niobate (PPLN), Prism (P), Germanium filter (Ge), Optical shutter (OS), Off Axis Parabolic (OAP), Cell detector (CD), Amplitude Modulation detector (AMD), Reference Detector (RD), Reference Cell (RC), Cell Window (CW), and Multi Pass Mirror (MPM).

In order to obtain high sensitivities, the amplitude, shape, and time dependence of the noise signals on the Amplitude Modulation detector (AMD) must be matched to that emanating from the CD in a robust manner. Since this noise is in the mid 10^{-4} to 10^{-3} absorbance range, and one requires ultimate absorbance sensitivities less than 10^{-6}, the noise on the AMD must be matched to the noise captured by the CD to better than 1 part in 1000. Furthermore, as our system employs second harmonic detection using phase sensitive detection, the phase of the detected signals must be closely matched in the two detection chains. To achieve these stringent requirements the present study addressed the following areas: 1) matching of the illuminated detection areas and beam shapes on the AMD and CD; 2) elimination of scattered light that may not be equally captured by the two detectors; 3) accurate matching of the two detection channels in terms of ac and dc gain, phase, and this includes the detectors and lock-in amplifiers; 4) minimizing PPLN temperature variations, which tends to exacerbate shape differences of the detected signals on the AMD and CD; 5) applying active wavelength control and; 6) balancing the inherent signal difference between the CD and AMD. By applying the above strategies a typical CH_2O sensitivity of 13 pptv (A_{min}~$4.3*10^{-7}$) is achieved for 60 s averaging during laboratory conditions. These results are a factor of 18 – 30 lower than achieved with our earlier DFG studies. However, by averaging for 260 seconds, which is not possible with the TDLAS, a sensitivity of 5 pptv (A_{min}~1.7×10^{-7}) is achieved. To our knowledge, such performance is the highest achieved with a DFG-based system.

The laboratory DFGAS was subsequently modified and operated onboard NCAR's C-130 airplane during the 2006 MIRAGE/IMPEX campaigns. To our knowledge, these are the first airborne demonstrations of a DFG system in the world. Typical airborne LODs for CH_2O during the second campaign produced 1-second and 1-minute median values of 100 pptv and 21 pptv, respectively. Although quite similar to our present TDLAS performance, a number of improvements have been identified, and these will be discussed in the oral presentation.

ACKNOWLEDGEMENTS

The National Center for Atmospheric Research (NCAR) is sponsored by the National Science Foundation (NSF). In addition to core funds from NSF this work was partially funded by the NOAA Climate and Global Change Program and the NASA Tropospheric Chemistry Program.

REFERENCES

1. A. Fried and D. Richter, Chapter 2 "Infrared Absorption Spectroscopy", in *Analytical Techniques for Atmospheric Measurement,* D.E. Heard (ed.) Blackwell Publishing, Oxford, UK, 2006.
2. A. Fried, B. Henry, B. Wert, S. Sewell, and J.R. Drummond, "Laboratory, ground-based, and airborne tunable diode laser systems: Performance characteristics and applications in atmospheric studies", Appl. Phys. **B 67,** 317 – 330, 1998.
3. A. Fried, B. Wert, B. Henry, J.R. Drummond, G. Frost, and Y.-N. Lee, "Airborne tunable diode laser measurements of formaldehyde during the 1997 North Atlantic Regional Experiment", SPIE Proceedings, Denver, CO, **3758,** 90 – 99, 1999.
4. A. Fried, et al., "Tunable diode laser measurements of formaldehyde during the TOPSE 2000 study: Distributions, trends, and model comparisons" J. Geophys. Res., **08** (D4), doi:10.1029/2002JD002208, 2003.
5. B.P. Wert, M. Trainer, A. Fried, et al., "Signatures of Alkene Oxidation in Airborne Formaldehyde Measurements During TexAQS 2000", J. Geophys. Res., **108**, (D3), doi:10.1029/2002JD002502, 2003.
6. B.P. Wert, A. Fried, S. Rauenbuehler, J. Walega, and B. Henry, "Design and Performance of a Tunable Diode Laser Absorption Spectrometer for Airborne Formaldehyde Measurements", J. Geophys. Res., **108,** (D12), doi: 10.1029/2002JD002872, 2003.
7. A. Fried, et al., "Airborne Tunable Diode Laser Measurements of Formaldehyde During TRACE-P: Distributions and Box-Model Comparisons", J. Geophys. Res., **108** (D20), 8798, doi: 1029/2003/JD003451, 2003.

8. C. Roller, A. Fried, J. Walega, P. Weibring, and F. Tittel, "Advances in hardware, system diagnostics software, and acquisition procedures for high performance airborne tunable diode laser measurements of formaldehyde", Appl. Phys. **B 82,** 247 – 264, 2006.
9. C. Dyroff et al., "Herriott Cell for Trace Gas Measurements on Airborne Platforms", in *Conference Proceedings*, *OSA Laser Applications to Chemical and Environmental Analysis (LACEA)*, Annapolis, MD, 2004.
10. S.D. Sewell, A. Fried, B.E. Henry, and J.R. Drummond, "A Field Diode Laser Spectrometer Employing an Astigmatic Herriott Cell" Proc. SPIE **2112,** 72 - 80, 1993.
11. A. Fried, J.R. Drummond, B. Henry, and J. Fox, "Reduction of Interference Fringes in Small Multipass Absorption Cells by Pressure Modulation", Appl. Opt. **29,** 900 – 902, 1990.
12. P. Weibring, D. Richter, A. Fried, J.G. Walega, and C. Dyroff, "Ultra-High-Precision Mid-IR Spectrometer II: System Description and Spectroscopic Performance", Appl. Phys. **B** doi: 10.1007/s00340-006-2300-4, 2006.
13. D.G. Lancaster, A. Fried, B. Wert, B. Henry, F.K. Tittel, "Difference-Frequency-Based Tunable Absorption Spectrometer for Detection of Atmospheric Formaldehyde", Appl. Opt. **24**, 4436 - 4443, 2000.
14. D. Richter, A. Fried, B. Wert, J.G. Walega, F.K. Tittel, "Development of a Tunable Mid-IR Difference Frequency Laser Source for Highly Sensitive Airborne Trace Gas Detection", Appl. Phys. **B**, doi: 10.1007/s00340-002-0948-y, 2002.
15. D. Richter, and P. Weibring, "Ultra-High Precision Mid-IR Spectrometer I: Design and Analysis of an Optical Fiber Pumped Difference-Frequency Generation Source", Appl. Phys. **B,** doi: 10.1007/s00340-005-2072-2, 2005.

* Email: fried@ucar.edu; Phone: 303-497-1475; Fax: 303-497-8770